Vol 15 No 10, October 2006
1009-1963/2006/15(10)/2288-09

Chinese Physics

© 2006 Chin. Phys. Soc.
and IOP Publishing Ltd

The second dissociation threshold bound levels of hydrogen molecule

Zhang Yan-Peng(张彦鹏)[a)b)], Song Jian-Ping(宋建平)[a)], Gan Chen-Li(甘琛利)[c)], Yan Xiang-An(严祥安)[a)], Nie Zhi-Qiang(聂志强)[a)], Jiang Tong(姜　彤)[a)], Li Ling(李　岭)[a)], Du Kai(杜　凯)[a)], Zhang Xiang-Chen(张相臣)[a)], Lu Ke-Qing(卢克清)[d)], and E.E. Eyler[b)]

[a)] *Department of Electronic Science and Technology, Xi'an Jiaotong University, Xi'an* 710049, *China*
[b)] *Department of Physics, University of Connecticut, U-3046, Storrs, CT* 06269, *USA*
[c)] *Department of Physics, University of Arkansas, Fayetteville, AR* 72701, *USA*
[d)] *State Key Laboratory of Transient Optics and Technology, Xi'an Institute of Optics and Precision Mechanics, Chinese Academy of Sciences, Xi'an* 710068, *China*

(Received 29 May 2005; revised manuscript received 9 June 2006)

The near-threshold highly bound states of all three stable isotopic variants of molecular hydrogen have been studied. Numerous perturbations and unexpected transitions are observed as far as 1cm^{-1} just below the second dissociation threshold. This complex structure may arise from a combination of nonadiabatic coupling between B, B′, C electronic states, perturbations due to fine and hyperfine interactions, and strong shape resonances. The perturbed near-threshold states and vibrational continuum exhibit finegrained structure, differing greatly between isotopes because of varying nonadiabatic coupling.

Keywords: dissociation threshold, nonadiabatic coupling, bound states

PACC: 3380, 3315

1. Introduction

Hydrogen, the smallest neutral molecule, is considered an ideal test system for quantum calculations of energy levels in a bound molecular system. However, the hydrogen molecule is not the simplest system. The near-threshold structure (where the long-range interatomic potentials are dominant) is remarkably complex.[1−5] Using the superior resolution Rydberg detection scheme for the double-resonance spectroscopy, we first studied the threshold regions in H_2, D_2, and HD, including extremely long-range vibrational levels with binding energies as small as 0.7 cm^{-1} for H_2, 1.5 cm^{-1} for D_2, 2.7 cm^{-1} for HD, respectively, and outer turning points in excess of 100 bohrs. The near-threshold vibrational structure is very irregular because of long-range coupling between these various fine and hyperfine levels, as well as nonadiabatic mixing of the molecular configurations of the B, B′ and C states. The corresponding problem for alkali dimers has been studied extensively, because the highest vibrational levels are observed in the photonassociation spectra of ultracold atoms in magneto-optical traps. For such weakly bound states the perspectives of the molecular physics and atom collision theory are almost equally applicable. The investigations of cold and ultracold collisions of alkali–metal atoms in atom traps have revealed partially resolved resonant structure thought to arise from analogous weakly bond molecular levels. In order to better describe the long-range interaction in alkali–metals, several excited hyperfine structure levels with curve crossings at long range have been considered. Some of the unusual spectra and interactions described here will probably be typical of these other one-electron systems as well.

The B′ state with C_6/R^6 long-range behaviour correlates to $H(1s_{1/2})+H(2s_{1/2})$ limit adiabatically. However, the B state has C_3/R^3 long-range behaviour in the potential, converging into the $H(1s_{1/2})+H(2p_{1/2})$ limit adiabatically. The C state has long-range behaviour in the potential with the barrier correlating to $H(1s_{1/2})+H(2p_{3/2})$ limit adiabatically. Transitions from the EF states to the rovibrational levels of all three states are possible, though the adiabatic electric transition moments to the B state are of the order of magnitude weaker than that to the B′ or C states. However, the strong nonadiabatic

coupling between the B, B′, and C states allow the observation of the bound levels of the B state. The B state is quite unusual because its broad resonant dipole interaction C_3/R^3 long-range potential curve supports a relatively dense set of the high vibrational levels. In this paper, the fully resolved highest bound structures of H_2, D_2 and HD near the extreme dissociation limit are measured, in many cases even the natural linewidths are resolved. This measurement gives a reliable dissociation limit.[1−5]

2. Experiment

The determination of dissociation energy is the culmination of a multi-year effort,[1] involving three major experimental measurements: near threshold measurement, calibration of EF, $v = 6$ and $v = 9$, and new determination of the $v = 0$ levels of the EF state.[1] In this paper we only describe the highly bound states near the second dissociation threshold measured by the Rydberg detection scheme.

The near threshold experimental setup in Fig.1 is similar to that in Refs.[3] and [5]. Some details are not repeated in this paper although the essential part of the experiment is faithfully described. The experiment is performed with a pulsed supersonic beam of molecular hydrogen. Two or more lasers cross the molecular beam at right angles in the interaction region. The broadband UV pulses at 193 nm are generated by mixing the fourth harmonic of a Nd:YAG laser at 266 nm with a Nd:YAG pumped dye laser at 705 nm, with room temperature BBO. The UV pulse at 193 nm operates in a small number of longitudinal cavity modes, jumping erratically between them. Two photons at about 193 nm excite selected levels of the EF($v = 6$ or $v = 9$) state. Lifetimes of gerade states EF are typically 100–200 ns, indicating that optical transitions between excited states is indeed a dominant decay mechanism, whereas extreme ultraviolet fluorescence to the X or $b^3\Sigma_u^+$ states is forbidden by dipole or spin selection rules. After a typical 60-ns delay, a narrowband probe laser at 677 nm excites the molecules to the region of the second dissociation limit. A three-stage capillary dye amplifier, pumped by a Continuum YG681 injection-seeded Nd:YAG laser, is used to amplify a cw beam from a ring dye laser to generate the probe laser pulse. The resultant probe pulse with 6 ns in duration is focused into a typical diameter of 0.7 mm, and we vary its energy from 15 μJ to 2 mJ according to the strength of individual transitions. The obtainable resolution is determined by the transform-limited bandwidth of the 677-nm laser, approximately 90 MHz, and by the residual transverse Doppler width, approximately 25 MHz for our highest-resolution work.[2,6,7]

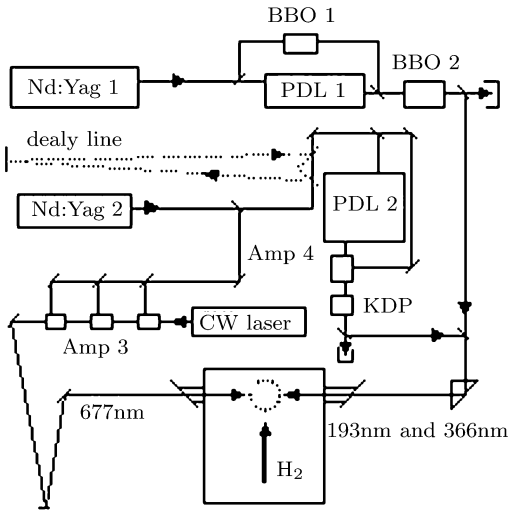


Fig.1. Threshold experimental setup of four detection schemes. PDL stands for a pulsed dye laser.

A pulsed laser is used to excite the EF states, and subsequently a high-resolution pulse-amplified laser is used to probe the region of the second dissociation limit. The excited hydrogen atoms produced by predissociation are detected with an auxiliary laser that drives the atomic 40p ← 2s and 40d ← 2p transitions, producing high Rydberg states that are easily detected by pulsed field ionization. Transitions to very high vibrational levels of the B, B′, and C states have been measured with a 0.002-cm^{-1} accuracy. Specifically, a pulsed dye laser with a bandwidth of about 0.5 cm^{-1} is operated at 732 nm (Fig.1). Its output is further amplified in a transverse dye cell, then frequency doubled in KDP to produce about 1mJ for a 6-ns pulse at 366 nm. The typical delay is 30 ns between the probe and the 366-nm UV detection laser. The $n = 2$ dissociation product can be excited to $n = 40$ Rydberg state of hydrogen atom by the 366-nm detection laser. Later, a delayed high voltage pulse is used to ionize the $n = 40$ hydrogen atom and detect the dissociation continuum. The bandwidth of this detection laser is about 0.5 cm^{-1}. Although the centre frequency of the detection laser is tuned to atomic Rydberg transition, some highly bound molecular states also can be excited to $n = 40$ molecular Rydberg state and de-

tected. One of the necessary requirements is that the binding energy must be comparable to the bandwidth of the detection laser. It should be noted that our method of detecting bound levels through Rydberg state has no selectivity in electronic character. The 2s hydrogen atom is metastable with a lifetime of about 1/7 s. On the other hand, the 2p lifetime is only 1.6 ns. To circumvent the difficulty of detecting species with short radiative lifetime, the probe and detection lasers are operated in coincidence for observing the highly bound molecules and 2p atoms. A 30-ns delay is introduced between the probe and the detection laser to detect 2s atoms. Limited by the finite bandwidth of the detection laser, the Rydberg detection scheme loses detection efficiency for those molecules bound deeper than 1 cm^{-1}. This Rydberg detection scheme significantly reduces the power requirements for the probe and detection lasers.[1] Therefore the power broadening is nearly eliminated and sensitivity is improved.

3. The second dissociation threshold bound levels

According to the binding energy relative to the $2s_{1/2}$+1s dissociation limit, we will divide the highly bound spectrum at the second dissociation limit into two regions: one is bound by less than 1 cm^{-1} and the other is bound more deeply. The detection method and the resolution strongly depend on the binding energy as one soon will realize. As a result, these two binding energy regions bear different significance in our discussion.

Due to the difference in selectivity and efficiency between different detection schemes, generally the H(2s+2p) detection through Rydberg state has the highest resolution and reveals more spectral details in the near-threshold region than other schemes. However, it is usually limited to those levels bound no more than 1 cm^{-1}. Because of the short radiative lifetime of the highly excited bound state, it cannot be observed well by detecting only the H(2s) atom through the Rydberg state. There is a 30-ns delay for the detection laser in that scheme, and only species whose lifetime is comparable to or longer than 30 ns can be observed. Figure 2(a) is a good example of the difference between H(2s) only and H(2s+2p) detections.

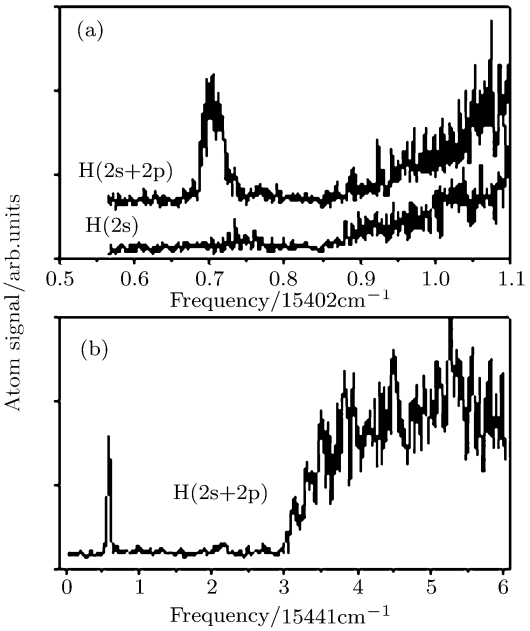


Fig.2. (a) The highest bound state in HD excited from $N" = 1$ EF($v = 6$) state, observed in different detection schemes. Both H(2s) and H(2p) are detected in the top trace but only H(2s) is detected in the bottom trace. The bound state can only be observed with H(2s+2p) detection. (b) The highest bound state and H(2s)+D(1s) continuum excited from $N" = 0$ EF($v = 6$) state of HD. Only H(2s +2p) is detected.

Although there exists a certain advantage of using Rydberg detection, it cannot be used to differentiate the highest bound state from the dissociation continuum in Figs.3 and 4. $H_2{}^+$ multiphoton ionization (MPI) is the alternative to detecting bound levels.

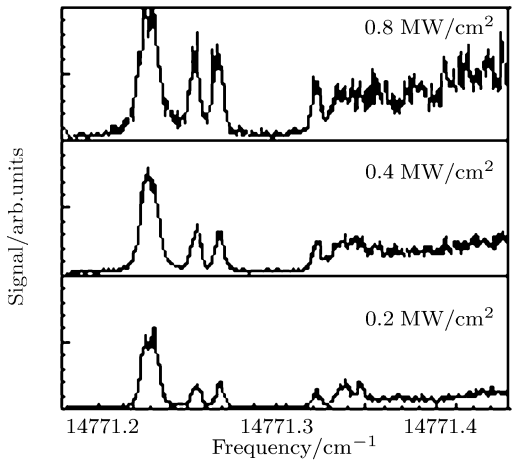


Fig.3. The ac Stark shifts and depletion broadening in H_2 from EF($v = 6$), $N'' = 1$, H(2s+2p) detection through Rydberg state is used.

Due to the bound state preference of the $H_2{}^+$ MPI detection scheme, continuum part of the spectrum will not be detected. In other words, we are able to determine all three features around 14771.3462 cm^{-1} to be bound levels instead of continuum structure. Although it is a good method to differentiate bound level

from continuum, the degradation of the spectral resolution is prominent due to the high power requirement of photoionization process. The H^+ detection of MPI requires even more photons and higher laser power than the $H_2{}^+$ MPI. However, it has no strong bias against the dissociation continuum. As a matter of fact, it was the preferred approach in the early study of dissociation limit and continuum structure before the Rydberg detection scheme was employed.[1]

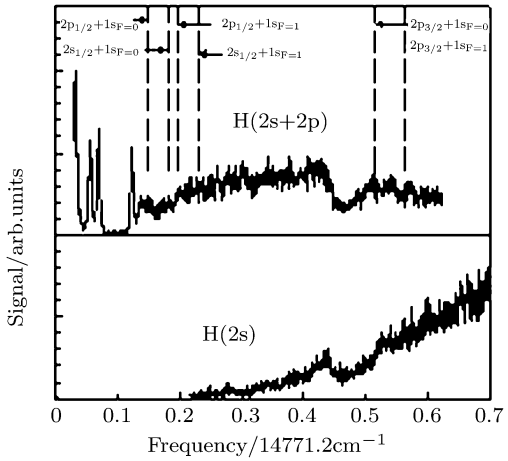


Fig.4. Interference due to the fine and hyperfine interactions in H_2 near-threshold continuum. Top trace is detected by H(2s+2p) scheme. The two highly bound states are depletion-broadened and mixed into the dissociation continuum. The bottom trace is detecting H(2s) only.

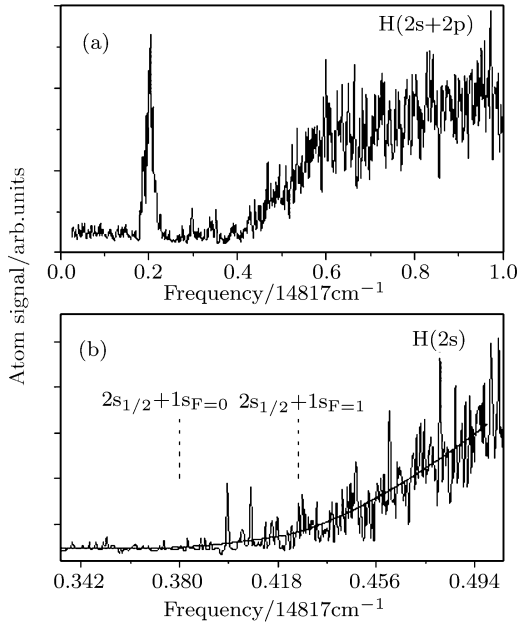


Fig.5. (a) The highest bound state and continuum excited from N" = 0, EF(v = 6) state in H_2, with H(2s+2p) detection scheme used. (b) H_2, continuum excited from N' = 0, EF(v = 6) state with H(2s) detection scheme used. The slope change of continuum at the 14817.425(25) cm^{-}1 of H($2s_{1/2}$)+H($1s_{F=1}$) threshold is due to the hyperfine interaction of H(1s) atom.

The Rydberg detection appears to be the best scheme for the levels bound by less than 1 cm^{-1}. In fact, the high resolution of the Rydberg detection also allows us to faithfully investigate the continuum structure. In Fig.5(a), the highest bound state and continuum are excited from $N'' = 0$, EF($v = 6$) state in $H_2{}^+$ with H(2s+2p) detection scheme used. Comparing with the measurements by using MPI detection scheme in Ref.[1], except the bound state 14817.2254(54) cm^{-1}, the other two highly bound states 14817.3125(30) cm^{-1} and 14817.3432(40) cm^{-1} are really weak. In this particular case, the sensitivity of the Rydberg detection is not so advanced.

The high resolution of the Rydberg detection method also enables us to measure the small power-dependence spectral shifts of some highest bound levels as demonstrated in Fig.6(a). The frequency and linewidth of the highest bound level in Fig.6(a) are

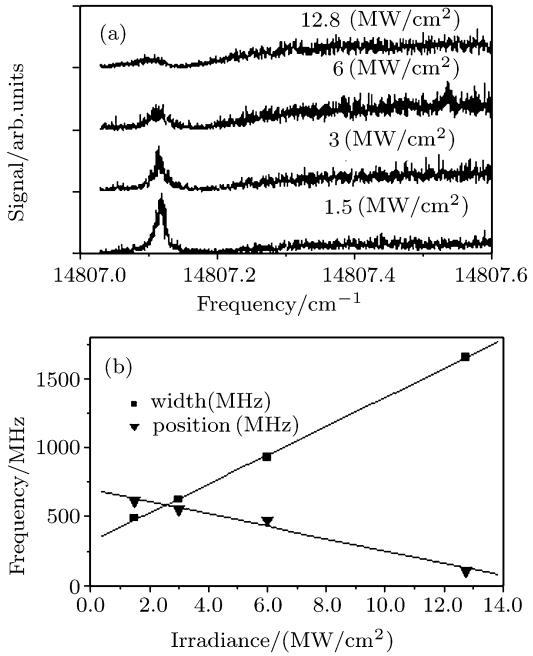


Fig.6. (a) The ac Stark effect for the B' (v = 13, N = 2) state in D_2. D(2s+2p) detection through Rydberg state is used. When the laser irradiance increases, the line centre is shifted toward lower laser frequencies and the line width increases. (b) The apparent width and line centre of B′ (v = 13, N = 2) state in D_2 as a function of laser irradiance. To determine the linewidth and the line centre, the best-fit lines are extrapolated to zero laser irradiance.

measured against the laser pulse energy. For those levels with sufficiently good signals, we find that the line centre and the line width generally depend on the laser pulse energy linearly as expected as a result of ac Stark effect. The intersection of zero laser energy and the best-fit line will gives the unperturbed line position and the linewidth as shown in Fig.6(b). The observed highly bound levels relative to EF (v = 6 or

$v = 9$) state are listed in Table 1. The highest bound level 14807.1270(22) cm^{-1} lies just 0.042(12) cm^{-1} below D($2s_{1/2}$)+D(1s) dissociation threshold, which we tentatively identify as B′, $v = 13$, $N = 2$. The ac Stark shifts are measured and corrected as described above. Generally speaking, the linewidths of those levels are much broader than the linewidth of our probe laser. This observation concludes that the lifetime of those highly excited states is shorter than the duration of laser pulse and confirms our earlier argument of detection strategy. The typical linewidth is measured to be more than 140 MHz for those detected highly bound levels. Note that deconvolution with laser bandwidth is necessary in order to yield the true spectral width.

Table 1. Excitation energies of highly bound levels from EF state and the X ($v = 0$, $N = 0$) ground state. Measurements are from $v = 6$ of EF state for H_2 and HD, and from $v = 9$ for D_2. $N'(N'')$ is the rotational quantum number.

Assignment	$N'(N")$	From EF state	Linewidth	Lifetime /ns	From X($v = 0$ $N = 0$) state	Binding energy
H2, B′($v = 9$)	1(0)	14817.2254(54)	0.0022(48)[a)]	3(5)	118376.8198(57)	0.189(24)
B($v = 39$)	1(0)	14817.3125 (30)	< 0.014[a)]	> 0.39[a)]	118376.9069(36)	0.102(23)
B($v = 40$)	1(0)	14817.3432 (40)	< 0.014[a)]	> 0.39[a)]	118376.9376(45)	0.071(23)
	0 or 2 (1)	14770.7381(67)	< 0.0296[a)]	> 0.18[a)]	118376.3479(70)	0.6808(72)
	0 or 2 (1)	14770.7521(24)	< 0.0193[a)]	> 0.28[a)]	118376.3619(31)	0.6668(36)
	0 or 2 (1)	14770.8730(31)	0.0048(32)	1.10(72)	118376.4828(37)	0.5459(41)
	0 or 2 (1)	14770.8844(39)	0.0093(31)	0.57(19)	118376.4942(44)	0.5345(48)
	0 or 2 (1)	14770.8985(33)	0.0081(35)	0.66(29)	118376.5083(38)	0.5204(42)
	0 or 2 (1)	14771.1440(21)	0.0023(33)	2(3)	118376.7538(29)	0.2749(34)
	0 or 2 (1)	14771.1558(21)	0.0061(32)	0.87(45)	118376.7656(29)	0.2631(34)
	0 or 2 (1)	14771.2264(21)	0.0039(31)	1(1)	118376.8362(29)	0.1925(34)
	0 or 2 (1)	14771.2314(21)	0.0041(31)	1.29(98)	118376.8412(29)	0.1875(34)
	0 or 2 (1)	14771.2555(21)	0.0044(30)	1.22(84)	118376.8653(29)	0.1634(34)
	0 or 2 (1)	14771.2688(21)	0.0039(30)	1(1)	118376.8786(29)	0.1501(34)
	0 or 2 (1)	14771.3257(20)	0.0026(30)	2(2)	118376.9355(28)	0.0932(34)
	0 or 2 (1)	14771.3370(21)	0.0057(36)	0.94(60)	118376.9468(29)	0.0819(34)
	0 or 2 (1)	14771.3462(24)	0.0023(38)	2(4)	118376.9560(31)	0.0727(36)
D2, B′($v = 13$)	1(0)	14831.5613(39)	0.0161(38)	0.33(8)	119028.1943(41)	1.488(15)
B($v = 52$)	1(0)	14831.7465(62)	0.0000(42)		119028.3795(64)	1.303(16)
B'($v = 13$)	2(1)	14807.1270(22)	0.0108(42)	0.49(19)	119029.6344(27)	0.042(12)
H*D, B′($v = 10$)	1(0)	15441.6022(67)	< 0.0267[a)]	> 0.2[a)]	118662.4160(86)	2.361(22)
B($v = 43$)	0 (1)	15400.1794(66)	0.0390(31)	0.14(1)	118662.091(41)	2.693(17)
B($v = 43$)	2 (1)	15401.3849(66)	0.014(30)	0.39(86)	118663.296(41)	1.487(17)
B'($v = 10$)	2 (1)	15402.6895(58)	0.0091(37)	0.58(23)	118664.601(40)	0.182(17)

[a)] Insufficient data for power extrapolation.

Absolute term energies of highly bound levels relative to the ground state X ($v = 0$, $N = 0$) are determined by adding three terms together. The first is the observed transition energies from EF ($v = 6$ or $v = 9$) in Table 1. The second is our newly calibrated energy intervals of EF, $v = 6$ for H_2 and HD, and $v = 9$ for D_2 from $v = 0$.[1] The third is the EF ($v = 0$) state term energies.[1] Combining uncertainties of these three terms in quadrature, we find the total uncertainties for the term energies of the highly bound state to be typically about 180 MHz. However, there are exceptions of those spectral lines in HD molecule excited from the $N'' = 1$ EF ($v = 6$) state. Their uncertainty of 0.04 cm^{-1} mainly stems from the uncertainty of EF, $v = 6$ calibration in HD.[1] Table 1 also lists the binding energies for the highly bound states of H_2, D_2 and HD, relative to the second dissociation $2s_{1/2}$+1s limit. Since both dissociation continuum and highly excited states are excited from a common EF state, the binding energies are calculated by subtracting the observed transition energies of the highly excited states, in Table 1, from the $2s_{1/2}$+1s dissociation thresholds. Since the H($2p_{1/2}$)+H(1s) threshold of H_2 is measured much more accurately than

the $H(2s_{1/2})$+H(1s) threshold of H_2,[1] we use the deduced, instead of directly measured, $H(2s_{1/2})$+H(1s) threshold of H_2 to calculate the binding energies for those bound states excited from the $N'' = 1$ EF state of H_2. The deduced $H(2s_{1/2})$+H(1s) threshold of H_2 is the measured $H(2p_{1/2})$+H(1s) dissociation threshold plus the well-known lamb shift 0.035 cm^{-1}. The binding energies are listed in the last column of Table 1. The uncertainties of dissociation threshold and transition energy are added together in quadrature, to calculate the combined uncertainty for the binding energy.

We are able to detect 22 of the 24 highly bound levels in Table 1 by the Rydberg detection scheme. The two more deeply bound levels at 15400.1794(66) cm^{-1} and 15401.3849(66) cm^{-1} that are excited from $N'' = 1$ level of EF($v = 6$) state of HD are detected by the MPI scheme. For excitation to states that are bound by more than 1 cm^{-1}, the Rydberg detection scheme is not reliable. The H_2^+ and H^+ detections are better strategies for those more deeply bound lines.[3] Among three isotopomers, H_2 has the richest bound spectrum in the near-threshold region. Seventeen lines are all observed by the Rydberg detection with high resolution, within 1 cm^{-1} of the dissociation limit for all rotations with $N' \leq 2$. By comparison, only one bound level at 14807.1270(22) cm^{-1} in D_2 is observed within the linewidth of our detection laser, and it is excited from $N'' = 1$ level of EF($v = 9$) state of D_2. HD also has one bound level observed at 15402.6895(58) cm^{-1} and within 1 cm^{-1} of the dissociation onset, which is excited from the $N'' = 1$ level of EF($v = 6$) state. Meanwhile, there are two highly bound levels of D_2 and $N' = 1$ observed with binding energies slightly larger than the linewidth of our detection laser at 14831.5613(39) cm^{-1} and 14831.7465(62) cm^{-1}. Even more surprisingly, there is an incident of observing a bound level 2.361(22) cm^{-1} lower than the dissociation onset 15443.963(21) cm^{-1} by H(2s+2p) detection through Rydberg state. It is the highest bound level 15441.6022(67) cm^{-1} excited from $N'' = 0$ of EF($v = 6$) state of HD as shown in Fig.2(b). Although detection slightly beyond the nominal bandwidth of the detection laser is acceptable with much reduced strength, detecting bound level about 1.86 cm^{-1} below the bandwidth is very unlikely. However, the observation can be explained by accidental excitation and ionization of $n = 39$ Rydberg state. Although the peak of the detection laser is tuned to the atomic transition between $n = 2$ and $n = 40$, it will also excite $n = 39$ Rydberg state if the binding energy of the bound level matches the energy interval between $n = 39$ and $n = 40$ Rydberg states within the detection limits of the detection laser. Note that the energy interval between $n = 39$ and $n = 40$ Rydberg states is about 3.56 cm^{-1}. Since the 400 V/cm detection field pulse is capable of ionizing any Rydberg state higher than $n = 35$, the $n = 39$ Rydberg state can be readily detected.

The highly bound levels listed in Table 1 should include only the B and B′ states without predissociative levels of the C state, namely those levels with $N' \geq 2$ of C-EF($v = 13$, $N = 6$) band above the dissociation limit in H_2.[4] Even armed with the selection rules, unfortunately, the uncertainty of assigning the rotational quantum number N' to 0 or 2 still exists when the intermediate EF($v = 6$ or $v = 9$) state has a rotation of $N'' = 1$. Tentative assignment of lines near the second dissociation limit has been given in Table 1. The highly bound levels of H_2 have dramatic exotic behaviour as indicated clearly by the fact that more transitions are observed than the expected. At this point, the accurate state assignment is not possible. The complex spectrum near the dissociation threshold, still not fully understood, arises from the combination of nonadiabatic coupling between B, B′, C electronic states, perturbations due to fine and hyperfine interactions, and strong shape resonances. This threshold physics is more complicated than in alkali dimmers. A detailed investigation of the perturbed structure in this energy range remains the subject of future work.

The calculations based on adiabatic mixing would fail due to the fact that nonadiabatic couplings extensively mix the electronic configurations of the B, B′, and C states. This mixing is apparent both in experimental results, where very strong transitions to the B state are observed,[3] and in nonadiabatic calculations exhibiting numerous bound levels. To accurately describe the highly bound levels, a complete Hamiltonian of the region very near threshold must include the fine and hyperfine interactions, as well as the Lamb-shift splitting between the 2s and 2p dissociation limits. To our knowledge, such a calculation has not yet been undertaken.

Using the MPI detection scheme, Fig.3 in Ref.[3] shows the binding energies of the observed levels closest to the second dissociation limit of H_2, together with previously assigned levels of the B′ and C states and the predicated positions of the highest B state levels.[3,5] They show that all possible singlet unger-

ade levels in this energy region are included in the predicted spectrum. Six transitions are observed with binding energies between 12 cm^{-1} and 41 cm^{-1} relative to the second dissociation onset, which agree well with calculated energies and confirm the strong mixing between the B, $v = 36$ or $v = 37$ levels and the B′, $v = 8$ level predicated by the nonadiabatic calculations.[3] The predicted and observed spectra begin to differ significantly about 12 cm^{-1} below threshold, at first with the appearance of extra lines in at least four cases, and finally with the complete breakup of the vibrational sequence in the last 1 cm^{-1} by MPI detection scheme. It is worth mentioning that our new results in Table 1 are more accurate than the measurements in Ref.[3]. Seventeen transitions are observed instead of seven transitions in the same last 1 cm^{-1} below the threshold of H_2, and the previous measurements must be interpreted as a blended lines. Three lines of parahydrogen are in reasonable agreement with the previous measurements, while the comparison is completely broken in orthohydrogen. The main structure of 14 lines maybe consists of 5 groups of lines, which are excited from $N'' = 1$ level of EF($v = 6$) state of H_2. Figure 3 shows seven lines of two groups near the extreme dissociation limit, with respect to two previous blended lines 14771.225(16) cm^{-1} and 14771.339(15) cm^{-1},[3] respectively. The double weak lines 14771.1440(21) cm^{-1} and 14771.1558(21) cm^{-1} are first resolved as another group in orthohydrogen. Table 1 also lists five strong transitions of two groups with larger binding energies, corresponding to two previous blended lines 14770.751(12) cm^{-1} and 14770.894(10) cm^{-1} in orthohydrogen,[3] respectively.

The irregular behaviour within 1 cm^{-1} of the limit is expected in hydrogen, because the vibrational spacing in this region is comparable in scale to the fine-structure and Lamb-shift interactions in the $n = 2$ H atom. The double lines seem much more surprising and can only arise from admixture of the singlet ungerade levels with other levels that are nearly degenerate. The repeated occurrence of this doubling suggests that the perturbing state must have a long-range potential curve nearly identical to the B state. A study of the interatomic potentials shows only one candidate $a(2s\sigma)^3\Sigma_g^+$, the triplet gerade potential curve arising from the same 1s+2p limit. In the absence of spin–orbit interaction, the triplet states have at long range exactly the same R dependence as the singlet states, twelve electronic states correlated with the second dissociation limit, of which six are triplet states, and hence the curves of the $GK^1\Sigma_g^+$, $C^1\Pi_u$, $B'^1\Sigma_u^+$, $EF^1\Sigma_g^+$, $\Pi'^1\Pi_g$, and $B^1\Sigma_u^+$ states resemble the curves of the $f^3\Sigma_u^+$, $i^3\Pi_g$, , $h^3\Sigma_g^+$, $e^3\Sigma_u^+$, $c^3\Pi_u$, and $a^3\Sigma_g^+$ respectively, all doubly degenerated. In view of the very small spin–orbit interaction in hydrogen the potential energy curves for the triplet states at long range still coincide with those of the singlets. Only at binding energies well below 1 cm^{-1} the difference becomes significant. However, the 14 dense bound levels with tiny binding energies in Table 1 seem to arise from the degeneracy of the a or h triplet gerade states and the much stronger B or B′ singlet ungerade states in last 1 cm^{-1} threshold region of orthohydrogen, respectively.

The only perturbation that can give rise to the normally forbidden admixture of these states is the hyperfine interaction. The hyperfine-induced g–u coupling term is typically similar in magnitude to the atomic hyperfine splitting. This term can be evaluated explicitly when the molecular wavefunction can be written as a simple combination of atomic wavefunctions (not a good approximation here because the atomic fine structure is strongly mixed). This interaction breaks down the g–u symmetry in any isotopomer but is rather weak: < 0.1 cm^{-1} for H_2 and < 0.2 cm^{-1} for HD at the second dissociation limit.[1] However, the separation between two highly bound spectral lines of H_2 in Table 1 is typically 0.01 cm^{-1}. In H_2 a nonadiabatic splitting of the dissociation limit occurs as a result of singlet–triplet interaction and the hyperfine structure, these splittings are small (≤ 0.3 cm^{-1}). Singlet–triplet interaction and u/g symmetry mixing are believed to cause the complex structure in H_2 but no quantitative theory could assign the lines observed.

Using the optical double resonance through the EF state, around the $n = 2$ limit four highly bound levels of HD have been observed with binding energies as small as 2.7 cm^{-1} in Table 1. Tentative reasonable assignment of four lines of HD has been made. The highest bound level 15402.6895(58) cm^{-1} lies just 0.182(17) cm^{-1} below dissociation threshold. The rovibrational levels very close to the dissociation limits for all singlet ungerade states have been observed.[1] For the B state band, origins are determined up to v = 43, very close to dissociation threshold, whereas vibrational levels up to v = 15 are observed for the C state. As for the B' state, levels are observed for $v = 0$ – 10. For the $v = 10$ levels with $N \geq 2$ levels are above the lower H^*+D limit; the N=4 level is even

above the second H+D* limit. A tentative assignment is given for B′ ($v = 11$, $N = 1$) at 118683.6 cm^{-1}. In HD no extra lines are observed in the optical double resonance through the B state, and the observed lines of g symmetry states lying just below the second dissociation threshold could be assigned unambiguously with a model that explicitly takes into account the g/u symmetry breaking. From such a perspective the HD molecule near the second dissociation limit, with a large splitting of 22.38 cm^{-1}, is easier to understand than H_2 molecule.

Stwalley[5] fitted and extrapolated the high vibrational levels of the B state by using an asymptotic expression for the adiabatic energies. However, McCormack and Eyler [3] calculated the second dissociation limit using $v = 37$ and $v = 38$ for H_2, and concluded that vibrational extrapolations should be approached very cautiously, since their region of validity is quite often limited. Unfortunately, now it is clear that the crucial $v = 39$ level of H_2 cannot be completely assigned in Table 1 and extrapolated to dissociation limit without a full analysis of fine and hyperfine interactions, and the previous assignment[3] must be interpreted as a blended line. Moreover, the approximate long-range model has to be applied to the constructed potential in HD with caution;[5,8] the R-dependent potential changes from C_3/R^3 to C_6/R^6 and the potential is well beyond the transition regime and follows almost exactly a C_6/R^6 function only for $v \geq 2$ of the I′ state.

Thus high-resolution laser spectroscopy has possibly led to the identification of most of the excited singlet u - symmetry states of the hydrogen molecule just below the second dissociation threshold, where most levels are narrow in the absence of autoionization and predissociation. The observed spectra with an accuracy of 0.01 cm^{-1} show the evidences for strong configuration mixing, hyperfine induced symmetry breaking, and a complete rearrangement of the spectrum very near the limit. Singlet-triplet interaction and u/g - symmetry mixing are believed to cause the complex structure in H_2 but no quantitative theory could assign the lines observed. Because so many interactions all play significant roles, they will probably have to be considered together for a successful theoretical treatment. One possibility is to employ the generalized multichannel quantum defect theory. Once the structure is fully understood, an accurate determination of the dissociation energy by vibrational extrapolation should be possible.

3.1. The EF($v = 0$) state term energies

Finally, the energy levels of $v = 6$ for H_2 and HD, and $v = 9$ for D_2 levels of EF state in Table 2, relative to the ground state are found from the calibration of EF, $v = 6$ and $v = 9$, relative to $v = 0$ by adding the EF(v =0) state term energies with an uncertainty of 0.0008 cm^{-1}.[1] The weighted average of two term energies for EF ($v = 9$, $N = 0$) state of D_2 is 104196.6330(15) cm^{-1}. Also the weighted average of two term energies for EF ($v = 9$, $N = 1$) state of D_2 is 104222.5074(15) cm^{-1}.

Table 2. EF state ($v = 6$ for H2 and HD, and $v = 9$ for D_2) term energies, relative to X($v = 0$, $N = 0$).

	Term energies
H_2 EF ($v = 6$, $N = 0$)	103559.5944 (19)
H_2 EF ($v = 6$, $N = 1$)	103605.6098 (20)
D_2 EF ($v = 9$, $N = 0$)	104196.6325 (21)
D_2 EF ($v = 9$, $N = 0$)	104196.6335 (20)
D_2 EF ($v = 9$, $N = 1$)	104222.5082 (22)
D_2 EF ($v = 9$, $N = 1$)	104222.5067 (21)
HD EF ($v = 6$, $N = 0$)	103220.8138 (55)
HD EF ($v = 6$, $N = 1$)	103261.911(40)

4. Conclusions

The very high resolution bound state spectra of molecular hydrogen can be obtained at the second dissociation limit to H(1s) + H(2s or 2p) by detecting the atomic products of dissociation. A pulsed UV laser excites transitions to the EF state, from which a second laser excites the bound or continuum states near the dissociation limit, and finally a third laser resonantly detects the hydrogen atoms. In favourable cases, the onset of the vibrational continuum can be located as accurately as 0.0027 cm^{-1} subject to the fully resolved highest bound states. The observed spectra in the last 1 cm^{-1} just below the second dissociation threshold show the evidences for strong configuration mixing, hyperfine induced symmetry breaking, and a complete rearrangement of the spectrum very near the limit. Because so many interactions all play significant roles, they will probably have to be considered together for a successful theoretical treatment.

References

[1] Zhang Y P, Cheng C H, Kim J T, Stanojevic J and Eyler E E 2004 *Phys. Rev. Lett.* **92** 203003

[2] Farooqi S M, Tong D, Krishnan S, Stanojevic J, Zhang Y P, Ensher J R, Estrin A S, Boisseau C, Cote R, Eyler E E and Gould P L 2003 *Phys. Rev. Lett.* **91** 183002
Tong D, Farooqi S M, Stanojevic J, Krishnan S, Zhang Y P, Cote R, Eyler E E and Gould P L 2004 *Phys. Rev. Lett.* **93** 063001

[3] McCormack E F and Eyler E E 1991 *Phys. Rev. Lett.* **66** 1042

[4] Eyler E E and Melikechi N 1993 *Phys. Rev.* A **48** R18

[5] Stwalley W C 1970 *Chem. Phys. Lett.* **6** 241

[6] Zhang Y P, de Araujo C B and Eyler E E 2001 *Phys. Rev.* A **63** 043802

[7] Zhang Y P, Gan C L, Li C S, Lu K Q, Hou X and Stanojevic J 2004 *J. Phys. B: At. Mol. Opt. Phys.* **37** 1751

[8] Chen J X and Gong Q H 2005 *Chinese Physics* **14** 1960

Chen Z Y, Qu W X and Xu Z Z 2000 *Chinese Physics* **9** 577

Zhang Y P, Lu K Q, Wu H C, Xu J and Fu P M 2000 *Chinese Physics* **9** 606